EMG Based Approach for Wearer-centered Control of a Knee Joint Actuated Orthosis

Walid Hassani, Samer Mohammed, Hala Rifaï and Yacine Amirat

Abstract— This paper presents a new human-exoskeleton interaction approach to provide torque assistance of the lower limb movements upon wearer's intention. The exoskeleton interacts with the wearer; the shank-foot orthosis system behaves as a second order dynamic system with gravity and elastic torque balance. The intention of the wearer is estimated by using a realistic musculoskeletal model of the muscles actuating the knee joint. The identification process concerns the inertial parameters of the shank-foot, the exoskeleton and the musculotendon parameters. Real-time experiments, conducted on a healthy subject during flexion and extension movements of the knee joint, have shown satisfactory results in terms of tracking error, intention detection and assistance torque generation. This approach guarantees asymptotic stability of the shank-foot-exoskeleton and adaptation to human-exoskeleton interaction. Moreover, the proposed control law is robust with respect to external disturbances.

I. INTRODUCTION

Recently, functional assistance-based robots have gained a particular attention as they are seen as an alternative to physiological (endurance) and psychological (repetitive tasks) limitations [1]. They are widely used in the medical domain, mainly for the functional rehabilitation; and in the military field to improve the endurance and to augment the physical forces [2]. They are often called exoskeleton or motorized orthoses in the medical domain. Exoskeletons are mechanical structures that embody the human limbs to ensure functional assistance during rehabilitation or during movement restoration of everyday activities. Exoskeletons should have suitable design able to ensure smooth cognitive and physical interaction with the wearer. Ideally, the exoskeleton should respond with precision to the intention of the wearer. Most of the current works focus mainly on the mechanical aspects of exoskeletons in order to optimize the effort transfer and to improve the wearer's comfort and ergonomy. The human-exoskeleton interface consists of two parts: the first one is physical and concerns measurement of the force interaction between the exoskeleton and the wearer. The second one is cognitive and concerns the control, based on the sensor information measured from the wearer such as kinematics (electrogoniometers), muscular activities (EMG), torque, ground interaction (baropodometric soles), etc. The force sensors are placed between the exoskeleton and the wearer to measure the interaction force. Impedance-based control laws are mainly used to ensure interaction between the wearer and the exoskeleton [3]. Effort-based strategies are often adopted because force sensors are easy to use and calibrate. Their main drawback concerns the time delay introduced in the closed loop control [5]. Moreover, it is not obvious to differentiate voluntary human efforts from external disturbances that may occur during the movement restoration process. On the other hand, EMG-based control laws are also used to control the wearable robots based on the measurements of the wearer's muscular activities. In [1], [4], a fixed upper limb exoskeleton is used to assist the flexion/extention movements of the elbow joint. The wearer's force is estimated from EMG signals and a simplified Hill-type muscle model is used along with neural networks. In [5], a knee joint exoskeleton controlled through the wearer's intention estimation is proposed. A musculoskeletal knee joint model is introduced to improve the estimation of the wearer's torque. In [6], the authors proposed a one DOF powered ankle foot orthosis with artificial pneumatic muscle for gait rehabilitation. The control schema is based on the assisting torque estimation by using a proportional controller as a function of the EMG activation level. In [7], an EMG interface is proposed to control two degrees of freedom exoskeleton. This exoskeleton assists flexion/extention and pronation/spination shoulder joint to perform predefined movements. The controller output is only adapted using raw EMG patterns previously learned using neuro-fuzzy model. In [8], raw EMG pattern recognition is used to control a two DOF wrist exoskeleton. A support vector machine is used to classify the EMG signals and to estimate the wearer's intention. The Hybrid Assistive Limb (HAL) relies on the detection of motion intention and the achievement of the movement task. The so-called voluntary control system estimates the wearer's intention through the detection of the nerve signals (EMG) [9], [10]. This paper lies in the continuity of previous works [11], [12]. However, in this study, instead of having a predefined position trajectory, the generated movement of the exoskeleton is based on the intention of the wearer and the dynamics of the interaction imposed through a stable control law. The rest of the paper is organized as follows: Section II presents the modeling of the shank-foot exoskeleton interaction dynamics as well as its parametric identification. Section III presents the proposed control law used to generate an appropriate exoskeleton torque with respect to the voluntary wearer muscular activities. Section IV shows the experiments as well as the robustness tests conducted on a healthy subject and section V presents the conclusion of this study.

W. Hassani, S. Mohammed, H. Rifa, and Y. Amirat are with the Laboratory of Images, Signals and Intelligent Systems (LISSI), University of Paris-Est Crteil, 122 Rue Paul Armangot, 94400 Vitry-Sur-Seine, France. E-mails: {walid.hassani, samer.mohammed, hala.rifai, amirat}@u-pec.fr

II. MODELING AND IDENTIFICATION

TABLE I
NOMENCLATURE

Variable	description
F_j^{mt}	Force of the jth musculotendon
ma_j	Moment arm of the jth musculotendon
RF	Rectus Femoris muscle
VL	Vastus Lateralis muscle
VM	Vastus Medialis muscle
VI	Vastus Intermedius muscle
ST	Semi-Tendinosus muscle
SM	Semi-Membranous muscle
BL, BS	Biceps femoris Long/Short head muscles
τ_{int}	Interaction torque between the exoskeleton and the wearer
τ_e, τ_h	Exoskeleton and human generated torques
$\theta_e, \dot{\theta}_e, \ddot{\theta}_e$	Exoskeleton angle, velocity and acceleration
$\theta_h, \dot{\theta}_h, \ddot{\theta}_h$	Knee joint angle, velocity and acceleration
$\theta_d, \dot{\theta}_d, \ddot{\theta}_d$	Desired knee joint angle, velocity and acceleration
θ_{re}, θ_{rh}	Exoskeleton and knee joint angles at rest position
J_e, J_h	Exoskeleton and shank-foot moments of inertia
K_e, K_h	Exoskeleton and knee joint stiffnesses
τ_{gh}, τ_{ge},	Exoskeleton and shank-foot gravitational torques
$a(t)$, $c(t)$	Muscle activation and Muscle excitation respectively [13]
τ_{act}, τ_{deact}	Activation and desactivation time constant
F_{max}	Maximum isometric muscle force
$f_l(\bar{l}_m(t))$	Force-length relationship [14]
$f_v(\bar{v}^m(t))$	Force-velocity relationship [15]
$\bar{l}^m(t), l_o^m$	Instantaneous normalized and optimal muscle lengthes
$\bar{v}^m(t), v_{max}^m$	Instantaneous normalized and maximal muscle velocities
γ	Shape factor of the force-length relationship
$\bar{b}^m$	Normalized damping coefficient
t, F^t	Time variable and Tendon force respectively
$l^t(t)$	Instantaneous musculo-tendon length
l_s^t	Musculo-tendon length at rest
S_c, k_v	Moment arm scale factor and shape factor respectively

A. Exoskeleton-Wearer Modeling
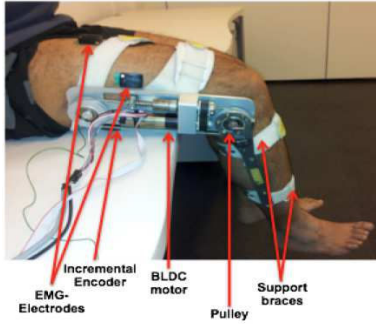
Fig. 1.   A person wearing the exoskeleton in a sitting position

In this study, the wearer is considered to be in a sitting position with the shank freely swinging (flexion and extension of the knee joint). $0°$ corresponds to full knee joint extension while $120°$ corresponds to maximum knee joint flexion. As shown in Fig.1, the exoskeleton has two segments coupled to each other at the knee joint level through a rotational axis. The upper segment embodies the thigh and supports the actuator while the lower one embodies the shank. The two segments are closely attached to the wearer lower limb through straps (Fig.1). The exoskeleton and the knee joint are supposed to have the same rotational degree of freedom in the sagittal plane. The shank-foot-exoskeleton is actuated by the exoskeleton, through the torque generated by the actuator τ_e, and the human torque generated by the wearer's muscles τ_h. The equation of movement of the exoskeleton is given as follows:

$$-\tau_{int} = \tau_e - (J_e\ddot{\theta}_e + B_e\dot{\theta}_e + K_e(\theta_e - \theta_{re}) + \tau_{ge}sin(\theta_e - \theta_{re})) \tag{1}$$

The equation of movement of the shank-foot is given as follows:

$$\tau_{int} = \tau_h - (J_h\ddot{\theta}_h + B_h\dot{\theta}_h + K_h(\theta_h - \theta_{rh}) + \tau_{gh}sin(\theta_h - \theta_{rh})) \tag{2}$$

Where:

$$\tau_h = \sum_{i=1}^{N} F_i^{mt}ma_i \tag{3}$$

The force generated by each skeletal muscle $F_i^{mt}, i \in \{1,\ldots,N\}$, is estimated using the modified Hill-type muscle [16]. In this study, the muscle's model is considered with a stiff tendon. The equations that govern the models of the generated muscular force, the muscular activation dynamics, the force-length and force-velocity relationships are given respectively as follows:

$$F^{mt}(t) = F_{max}\left[a(t)f_l(\bar{l}^m(t))f_v(\bar{v}^m(t)) + f_d(\bar{v}^m(t))\right] \tag{4}$$

$$\dot{a}(t) + \frac{1}{\tau_{act}}\left[\frac{\tau_{act}}{\tau_{deact}} + (1 - \frac{\tau_{act}}{\tau_{deact}})c(t)\right]a(t) = \frac{1}{\tau_{act}}c(t) \tag{5}$$

$$f_l(\bar{l}^m(t)) = \exp(-(\bar{l}^m(t) - 1)^2/0.45) \tag{6}$$

$$f_v(\bar{v}^m) = \begin{cases} \dfrac{0.3(\bar{v}^m(t)+1)}{-\bar{v}^m(t)+0.3} & \text{if } \bar{v}^m(t) \leq 0 \\ \dfrac{(2.34\bar{v}^m(t)+0.039)}{1.3\bar{v}^m(t)+0.039} & \text{if } \bar{v}^m(t) > 0 \end{cases} \tag{7}$$

$$f_d(\bar{v}^m(t)) = B^m\bar{v}^m(t) \tag{8}$$

The muscle lengths as well as the moment arms of each muscle actuating the knee joint are computed separately using a realistic musculoskeletal model that contains $N = 8$ muscles. 4 of them concern the quadriceps knee joint extensors, namely, the rectus femoris (RF), the vatus medialis (VM), the vastus lateralis (VL) and the vastus intermedius (VI). The remaining muscles correspond to the knee flexors, namely, the semi-tendinosus (ST), the semi-membraneous (SM), the biceps femoris long head (BL) and shorts head (BS). The insertion points of the considered muscles are taken from the anatomical data model [17].

B. Exoskeleton-Wearer interaction dynamics

When the wearer exerts a lower limb torque and the leg rotates of an angle $\delta\theta$ with respect to the exoskeleton in the sagittal plane. Then, the shank-foot rotation angle θ_h can be written as follows:

$$\theta_h = \theta_e + \delta\theta \qquad (9)$$

Equation (2) becomes:

$$\tau_{int} = \tau_h - \Big(J_h(\ddot{\theta}_e + \delta\ddot{\theta}) + B_h(\dot{\theta}_h + \delta\dot{\theta}) + K_h(\theta_e + \delta\theta - \theta_{rh}) + \tau_{gh}sin(\theta_e + \delta\theta - \theta_{rh})\Big) \quad (10)$$

The exoskeleton is supposed to be closely attached to the shank foot, thus, $\delta\theta$ is relatively small. Using Taylor expansion of order one, equation (10) can be expressed as follows:

$$
\begin{aligned}
\tau_{int} =& \ \tau_h - J_h\ddot{\theta}_e - B_h\dot{\theta}_h - K_h(\theta_e - \theta_{rh}) - \tau_{gh}sin(\theta_e - \theta_{rh})) \\
&- J_h\delta\ddot{\theta} - B_h\delta\dot{\theta} - K_h\delta\theta - \tau_{gh}cos(\theta_e - \theta_{rh})\delta\theta \quad (11)
\end{aligned}
$$

The interaction dynamics is obtained by substituting (10) in (1) and can be expressed as follows:

$$
\begin{aligned}
J_h\delta\ddot{\theta} + B_h\delta\dot{\theta} &+ K_h\delta\theta + \tau_{gh}cos(\theta_e - \theta_{rh})\delta\theta = \\
&\tau_e + \tau_h - (J_e + J_h)\ddot{\theta}_e - (B_e + B_h)\dot{\theta} \\
-(K_e + K_h)(\theta_e - \theta_{rh}) &- (\tau_{ge} + \tau_{gh})sin(\theta_e - \theta_{rh}) \qquad (12)
\end{aligned}
$$

III. PARAMETERS IDENTIFICATION

The identification procedure is performed with a healthy subject having the following features (Heigth=1.82 m, Weight=96 Kg, Sex=Male, Age=35 years old). The exoskeleton angle θ_e is measured using an incremental encoder while the exoskeleton generated torque τ_e is computed using the actuator current sensor. Both measurements, θ_h and τ_e, are filtered using a zero-lag fourth-order low-pass Butterworth filter characterized by a cutoff frequency of 3 Hz. Exoskeleton's angular velocity $\dot{\theta}_e$ and angular acceleration $\ddot{\theta}_e$ are derived numerically from the measured exoskeleton's angle. Step and chirp signals are used as knee joint desired trajectories. The identification process is done in two steps; the first one concerns the identification of the inertial parameters of both the wearer shank-foot and the exoskeleton while the second step concerns the identification of the muscle-tendon parameters. For more information regarding the identification procedure, the reader is pleased to refer to the following paper [18].

Four EMG sensors from Delsys^{TM} are used to measure the muscular activities of the following muscles: rectus femoris, vastus lateralis, semi-membranous/semi-tendinosus and biceps femoris long head/short head. Vastus Medialis (VM) Vastus Intermedius (VI) muscles are supposed to have the same excitation input as the Vastus Lateralis (VL) one. In order to remove movement artifact, EMG acquired data of the four muscles are filtered using a high-pass fourth-order recursive Butterworth filter with a cutoff frequency

TABLE II

LOWER LIMB MUSCULOSKELETAL PARAMETERS (-:IDENTIFIED, *:[19])

Muscle		$l_m^o(cm)$	$l_s^t(cm)$	$F_{max}(N)$	Sc
RF	-	8.6	34.2	748	0.95
	*	8.4	34.6	780	1
VL	-	8.3	16.2	1620	0.83
	*	8.2	15.7	1870	1
VM	-	8.2	11.8	1188	1.05
	*	8.9	12.6	1295	1
VI	-	7.8	12.7	1163	1.1
	*	8.7	13.6	1235	1
SM	-	7.93	40.5	992	0.84
	*	8	35.9	1030	1
ST	-	18.8	24.7	315	1.06
	*	20.1	26.2	330	1
BL	-	10.3	36	641	0.85
	*	10.9	34.1	720	1
BS	-	18.1	10.6	379	0.82
	*	17.3	10	413	1

equal to 30 Hz. The resulting signal is full wave rectified, and then filtered using a Butterworth low-pass filter with a 2 Hz cutoff frequency. The optimization is done offline using nonlinear least squares "Levenberg Marquardt" based algorithm. Elements of the χ vector have been initialized to values taken from the literature data reported in [19] and [17] except Sc that has been initialised to 1. Activation muscular dynamics parameters such as τ_{act} and τ_{deact} are taken from [13] and set to $0.02s$ and $0.06s$ respectively, the muscle maximum velocity v_{max} is set to $10l_o^m$, and the muscle damping B^m is set to 0.1 [20]. The identified parameters are shown in table II; one can note that the identified parameters and those taken from literature (physical quantity) are close and the difference lies within the tolerated physiological variation [21].

IV. EXOSKELETON CONTROL

The control of the exoskeleton is ensured upon the wearer's intention, determined through the EMG measurements of the shank muscle activities. The block diagram of the proposed control strategy is illustrated in Fig. 2. The desired knee joint angle is estimated based on (9) through the interaction dynamics given by (12) that are measured with respect to the wearer generated musculoskeletal torque. The proposed approach consists of applying a control torque that *i)* reflects the wearer intention, and *ii)* drives the exoskeleton to the desired knee joint angle. The first purpose is ensured by setting the wearer's knee joint angle θ_h as the desired angle to be tracked by the orthosis. The second purpose is reached by applying a control torque τ_e that allows the exoskeleton angle θ_e to track the desired human knee joint angle θ_h.

Define e as the angular error at the controller input. e is equal to the difference between the current exoskeleton angle θ_e and the desired knee joint angle θ_h ($e = \theta_e - \theta_h$). The angular velocity and acceleration errors are expressed respectively as follows: $\dot{e} = \dot{\theta}_e - \dot{\theta}_h$ and $\ddot{e} = \ddot{\theta}_e - \ddot{\theta}_h$.

Proposition 1: Consider the shank-foot-exoskeleton
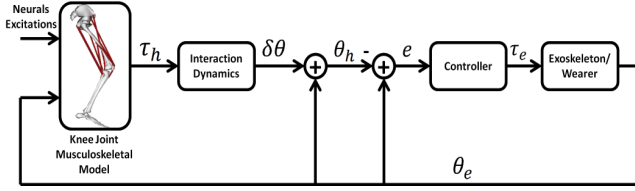
Fig. 2. Block diagram of the closed loop system

model described by (12). Consider that, at the rest position, the exoskeleton angle is equal to the knee joint one: $\theta_{rh} = \theta_{re} = \theta_r$. Define the control torque τ_e as follows:

$$
\begin{aligned}
\tau_e &= (J_e + J_h)\ddot{\theta}_d + (B_e + B_h)\dot{\theta}_d - K_i e - B_i \dot{e} \\
&\quad - \tau_{gh}\cos(\theta_e - \theta_r)e + (K_e + K_h)(\theta_e - \theta_r) \\
&\quad + (\tau_{ge} + \tau_{gh})\sin(\theta_e - \theta_r) \quad (13)
\end{aligned}
$$

with $B_i > 0$ and $K_i > K_h > 0$. The shank-foot-orthosis system subject to the control torque (13) and the human input torque τ_h is:

1. output strictly passive system, where the output is defined by $\dot{e}$,
2. finite gain L_2 stable.

If the human input torque $\tau_h = 0$, then the closed loop system is: a) zero-state observable and b) the origin $(e, \dot{e}) = (0,0)$ is asymptotically stable.

Proof: Firstly the tracking error e function of the interaction angle $\delta\theta$ is computed. Using (9), one can write:

$$
e = \theta_e - \theta_h = -\delta\theta \quad (14)
$$

Substituting (13) into (12), the closed loop dynamics becomes:

$$
\begin{aligned}
-(J_e + J_h)\ddot{e} - (B_e + B_h + B_i)\dot{e} - K_i e + \tau_h = \\
J_h \delta\ddot{\theta} + B_h \delta\dot{\theta} + K_h \delta\theta \quad (15)
\end{aligned}
$$

Replacing (14) into (15), one has:

$$
\begin{aligned}
(J_e + J_h)\ddot{e} + (B_e + B_h + B_i)\dot{e} + K_i e - \tau_h = \\
J_h \ddot{e} + B_h \dot{e} + K_h e \quad (16)
\end{aligned}
$$

Then:

$$
J_e \ddot{e} + (B_e + B_i)\dot{e} + (K_i - K_h)e = \tau_h \quad (17)
$$

A state space representation of (17) is given as follows:

$$
\begin{aligned}
\dot{x_1} &= x_2 \\
\dot{x_2} &= -\frac{(B_e + B_i)}{J_e}x_2 - \frac{(K_i - K_h)}{J_e}x_1 + \frac{1}{J_e}u \\
y &= x_2 \quad (18)
\end{aligned}
$$

where:

$$
x = [x_1, x_2]^T = [e, \dot{e}]^T \quad \text{and} \quad u = \tau_h \quad (19)
$$

Consider the positive definite radially unbounded Lyapunov candidate function V:

$$
V(x) = \frac{1}{2}J_e x_2^2 + \frac{1}{2}(K_i - K_h)x_1^2 \quad (20)
$$

V is continuously differentiable positive definite function and $V(x) = 0$ for $x = 0$. The time derivative of the Lyapunov function V is given as follows:

$$
\dot{V} = -(B_e + B_i)x_2^2 + x_2 u \quad (21)
$$

with:

$$
x_2 u \geq \dot{V} \qquad \forall(x_2, u) \in \mathbb{R} \times \mathbb{R} \quad (22)
$$

Moreover, there exists a scalar $\beta > 0$, such as:

$$
(B_e + B_i)x_2^2 \geq \beta \|x_2\|^2 \quad (23)
$$

Therefore:

$$
x_2 u \geq \dot{V} + \beta \|x_2\|^2 \quad (24)
$$

In view of (22) and $\beta\|x_2\|^2 > 0 \; \forall x_2 \neq 0$, (18) defines an output strictly passive system. Moreover, the system is finite gain L_2 stable and the L_2 gain is less than or equal to $1/\beta$:

$$
\|x_2\|_{L_2} \leq \frac{1}{\beta}\|u\|_{L_2}
$$

When the wearer is not generating any torque, i.e., $u = 0$, or developing a limited torque, u has therefore a finite energy, and tends to 0 when t tends to ∞ (muscular fatigue). When $u = 0$, (18) becomes:

$$
\begin{aligned}
\dot{x_1} &= x_2 \\
\dot{x_2} &= -\frac{(B_e + B_i)}{J_e}x_2 - \frac{(K_i - K_h)}{J_e}x_1 \\
y &= x_2 \quad (25)
\end{aligned}
$$

$y = 0$ is equivalent to $x_2 = 0$. Consequently, $\dot{x_2} = 0$ and $x_1 = 0$. The only solution of (25) for which the output is identically null is the trivial solution: $x = [x_1, x_2]^T = [0\ 0]^T$. Consequently, the closed loop system defined by the state space representation (18) is zero-state observable. Since the system is also output strictly passive, the state $x = [x_1, x_2]^T = [e, \dot{e}] = [0,0]^T$ is asymptotically stable and the exoskeleton angle θ_e converges to the knee joint angle θ_h determined upon the wearer's intention. ∎

V. EXPERIMENTAL RESULTS AND ROBUSTNESS TEST

The wearer is in a semi-supine sitting position, with the knee joint freely moving in the sagittal plane (flexion/extension). The experiments described in this section were performed by the same person who was subject to the identification procedure (see section III). The control scheme is tested online using the EICOSI (Exoskeleton Intelligently COmmunicating and Sensitive to Intention) exoskeleton, of the LISSI Laboratory of the University of Paris-Est Creteil (UPEC). The exoskeleton is actuated using a brushless DC motor (BLDC). This actuator has been chosen due to its relatively high torque/volume ratio. The exoskeleton is also equipped with an incremental encoder that measures the angle of the shank segment with respect to the thigh one. It is controlled through a PC using the dSPACE DS1103 controller board and the $Maxon^{TM}$ motion controller EPOS 70/10 that drives the brushless DC motor.
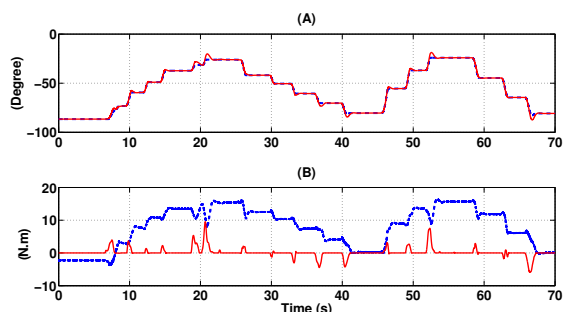
Fig. 3. Wearer performing step movements. (A) exoskeleton position (dashed blue line) and wearer desired position (red line), (B) exoskeleton developed torque (dashed blue line) and wearer developed torque (red line)
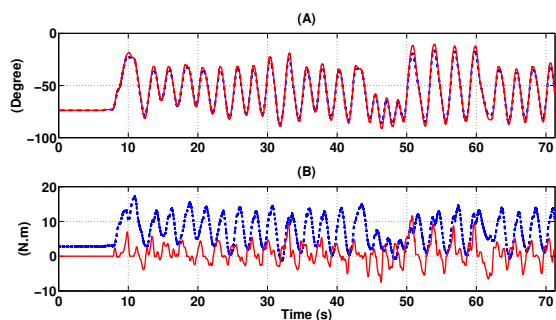
Fig. 4. Continuous movements. (A) exoskeleton position (dashed blue line) and wearer desired position (red line), (B) exoskeleton developed torque (dashed blue line) and wearer developed torque (red line)

In the following, we show the results corresponding to voluntary lower limb movements initiated by the wearer. These movements consist of repetitive flexion and extension of the knee joint. The wearer performs first consecutive desired steps of the knee joint in the flexion and extension directions (figure 3), and secondly, he performs continuous movements (figure 4). The exoskeleton driven through the control law described in section IV by (13) interacts with the wearer using the dynamic equation described by (17). The parameters of equations (2) and (1) are identified according to the method described in section III. Parameters of the control law as well as the interaction dynamics, K_i and B_i are empirically adjusted to obtain the best performances in terms of responsiveness of the exoskeleton to the wearer intention. The obtained parameters are $K_i = 75$ and $B_i = 6$.

Each of the figures 3, 4, 5 and 6, consists of two parts: part A shows the wearer's intended position computed through the dynamic model (full red line) and the current position of the exoskeleton (dashed blue line); part B shows the human generated torque (full red line), as well as, the torque developed by the exoskeleton (dashed blue line).

In figure 3, the time interval $[0-42]$ sec, shows a series of consecutive step movements with a range of approximately $10°$ towards the full knee joint extension. In the time interval $[42-70]$ sec, a consecutive knee joint flexion with an average of approximately 20 sec is shown. The figure 3 shows clearly that the exoskeleton's movement is triggered by the

wearer. One can notice also that once the desired position is reached, the human generated torque vanishes. The exoskeleton develops the necessary torque to maintain the shank-foot-exoskeleton at the desired position. Asymptotic convergence to the desired trajectory can be observed clearly in figure 3 at the moments 22 and 53 sec respectively.

Figure 4 shows the wearer performing continuous movements of flexion and extension. Amplitude of movements varies from $90°$ to $10°$ with a frequency that can reach 0.5 Hz. The exoskeleton tracks the estimated knee joint that reflects the wearer intention with an RMS error equal to $2.1799°$. These results show satisfactory interaction between the exoskeleton and the wearer. The necessary torque for a wearer to perform a similar movement, is equal to the sum of the torques generated by both the exoskeleton and the wearer. One can notice that, the exoskeleton supplies at least 50% of the necessary effort; and can supply until approximately 80% of the total effort, especially during the extension of the knee joint. These results show clearly that the exoskeleton provide functional assistance to the wearer during flexion and extension movements of the lower limb.

A. Robustness tests

In order to test the robustness of the proposed strategy with respect to uncertainties of the model parameters, an external load of 2 Kg has been attached at the wearer's foot level. This load has affected the inertia, elasticity and gravitational torque. As shown in figures 5-B and 6-B, the robustness tests show that despite the additional external load, the tracking performance as well as the interaction dynamics remain satisfactory using the same parameters: $K_i = 75$ and $B_i = 6$. We clearly observe that at moments 14, 19, 33, 45 and 48 seconds of figure 6, the current position of the exoskeleton converges asymptotically to the wearer's desired position. One can also notice satisfactory tracking performance (figure 6) with a RMS equal to 2.71 degrees. Nevertheless, one can notice from figures 3 and 6 that the wearer develop more efforts with respect to the experiments conducted without the additional load.
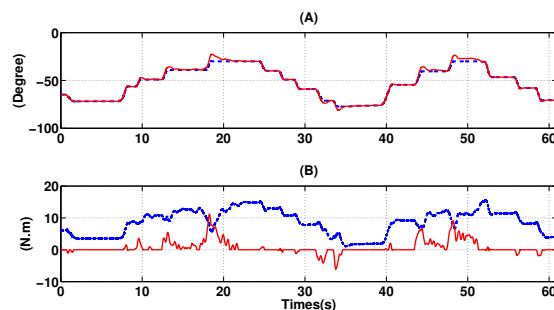
Fig. 5. Robustness tests for a wearer performing step movements. (A) exoskeleton position (dashed blue line) and wearer desired position (red line), (B) exoskeleton developed torque (dashed blue line) and wearer developed torque (red line)
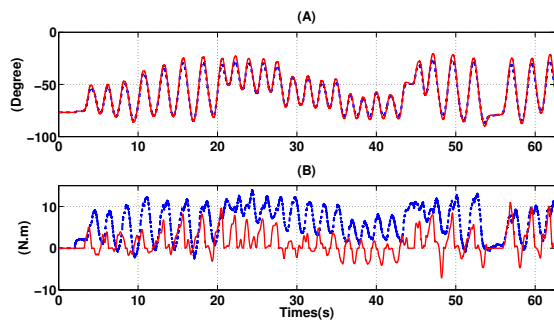
Fig. 6. Robustness tests for a Continuous movements. (A) exoskeleton position (dashed blue line) and wearer desired position (red line), (B) exoskeleton developed torque (dashed blue line) and wearer developed torque (red line)

VI. CONCLUSION

The present work concerns the development of a human-exoskeleton interaction model to assist movements of the wearer's lower limbs upon muscular activities measurements. The wearer's intention is estimated by using a realistic musculoskeletal model of the muscles actuating the knee joint. The proposed interaction model is used to provide position tracking of the wearer's desired position using the exoskeleton. The resulting closed loop system corresponds to a second order dynamic system with respect to the wearer generated torque. The proposed control law assists the wearer since it compensates the gravity and the passive torques induced by the shank-foot. The asymptotic stability has been proved using passivity theory. The advantage of the proposed approach lies in the fact that no predefined position trajectory is imposed to the wearer. The proposed control law is robust with respect to the identified parameters. Experimental validations were conducted on a healthy subject for knee joint movements flexion and extension. Satisfactory performances were observed in terms of position tracking and stable interaction between the wearer and the exoskeleton.

REFERENCES

[1] J. Rosen, M. Brand, M.B. Fuchs, and M. Arcan, *A myosignal-based powered exoskeleton system*, IEEE Transactions on Systems, Man and Cybernetics, Part A: Systems and Humans, Vol. 31-3, pp.210-222, 2001.

[2] S. Mohammed, Y. Amirat, and H. Rifai *An EMG-driven musculoskeletal model to estimate muscle forces and knee joint moments in vivo*, Advanced Robotics, Vol.26, 1-2, pp. 1-22, 2012.

[3] B. Siciliano and O. Khatib, *Springer handbook of robotics*, Springer, chapter 33, 2008.

[4] J. Rosen, M.B. Fuchs, and M. Arcan, *Performances of Hill-type and neural network muscle models-toward a myosignal-based exoskeleton*, Computers and Biomedical Research, Vol. 32-5, pp.415-439, 1999.

[5] C. Fleischer, and G. Hommel, *A Human–Exoskeleton Interface Utilizing Electromyography*, IEEE Transactions on Robotics, 24-2, pp.872-882, 2008.

[6] G.S. Sawicki, K.E. Gordon, D.P. Ferris, *Powered lower limb orthoses: applications in motor adaptation and rehabilitation*, 9th International Conference on Rehabilitation Robotics - ICORR, pp. 206-211, 2005.

[7] K. Kiguchi, K. Iwami, M. Yasuda, K. Watanabe, T. Fukuda, *An exoskeletal robot for human shoulder joint motion assist*, IEEE/ASME Transactions on Mechatronics, Vol.8-1, pp.125-135, 2003.

[8] Z.O. Khokhar, and Z.G. Xiao, and C. Menon, *Surface EMG pattern recognition for real-time control of a wrist exoskeleton*, Biomedical engineering online, Vol.9-1, pp. 41, 2010.

[9] T. Kawabata, H. Satoh, and Y. Sankai, *Working posture control of robot suit HAL for reducing structural stress*, IEEE International Conference on Robotics and Biomimetics - ROBIO, pp. 2013-2018, 2009.

[10] K. Suzuki, G. Mito, H. Kawamoto,Y. Hasegawa, and Y. Sankai, *Intention-based walking support for paraplegia patients with Robot Suit HAL*, Advanced Robotics, Vol. 21-12, pp.1441-1469, 2007.

[11] H. Rifai, W. Hassani, S. Mohammed and Y. Amirat, *Bounded control of an actuated lower limb orthosis*, IEEE International Conference on Decision and Control and European Control Conference (CDC-ECC), pp. 873- 878, 2011.

[12] H. Rifai, S. Mohammed, B. Daachi and Y. Amirat, *Adaptive Control of a Human-Driven Knee Joint Orthosis*, IEEE International Conference on Robotic and Automation - ICRA, pp.2486-2491, 2012.

[13] G.T. Yamaguchi, *Dynamic modeling of musculoskeletal motion: a vectorized approach for biomechanical analysis in three dimensions*, Kluwer Academic Publishers Norwell, MA, 2001.

[14] D.G. Thelen, *Adjustment of muscle mechanics model parameters to simulate dynamic contractions in older adults*, Journal of Biomechanical Engineering, Vol. 125-1, pp.70-77, 2003.

[15] L.M. Schutte, *Using Musculoskeletal Models to Explore Strategies for Improving Performance in Electrical Stimulation-induced Leg Cycle Ergometry*, Stanford University, 1993.

[16] M. Sartori, DG. Lloyd, M. Reggiani and E. Pagello, *A stiff tendon neuromusculoskeletal model of the knee*, IEEE Workshop on Advanced Robotics and its Social Impacts (ARSO), pp. 132-138, 2009.

[17] S.L. Delp, J.P. Loan, M.G. Hoy, F.E. Zajac, E.L. Topp, and J.M. Rosen, *An interactive graphics-based model of the lower extremity to study orthopaedic surgical procedures*, IEEE Transactions on Biomedical Engineering, 37-8, pp. 757-767, 1990.

[18] W. Hassani, S. Mohammed and Y. Amirat, *Real-Time EMG driven Lower Limb Actuated Orthosis for Assistance As Needed Movement Strategy*, Robotics: Science and Systems Conference - RSS'13, Berlin Germany, 2013.

[19] E.M. Arnold, S.R. Ward, R. L. Lieber, and S.L. Delp, *A model of the lower limb for analysis of human movement*, Annals Biomedical Engineering, 38(2), pp.269-79, 2010.

[20] F.E. Zajac, *Muscle and tendon: properties, models, scaling, and application to biomechanics and motor control*, Critical reviews in biomedical engineering, Vol. 17-4, pp.359, 1989.

[21] D.G. Lloyd, and T.F. Besier, *An EMG-driven musculoskeletal model to estimate muscle forces and knee joint moments in vivo*, Journal of biomechanics, Vol.36-6, pp. 765-776, 2003.